

# 000 001 002 003 004 005 006 007 008 009 010 011 012 013 014 015 016 017 018 019 020 021 022 023 024 025 026 027 028 029 030 031 032 033 034 035 036 037 038 039 040 041 042 043 044 045 046 047 048 049 050 051 052 053 VALUE SHAPING: BIAS REDUCTION IN BELLMAN ER- ROR FOR DEEP REINFORCEMENT LEARNING

Anonymous authors

Paper under double-blind review

## ABSTRACT

The Bellman error plays a crucial role as an objective function in deep reinforcement learning (DRL), serving as a proxy for the value error. However, this proxy relationship does not guarantee exact equivalence between the two, as the Bellman error inherently contains bias that can lead to unexpected optimization behavior. In this paper, we investigate the relationship between the value error and the Bellman error, and analyze why the Bellman error is not a reliable proxy due to its inherent bias. Leveraging the linear structure of the Bellman equation, we propose a value shaping method to compensate for this bias by adjusting the reward function—while ensuring that such modifications do not alter the optimal policy. In practice, we initialize two parallel Bellman iteration processes: one for estimating the bias and the other for updating the value function with minimal bias. Our method effectively learns a low-bias Q-function, making it broadly applicable and easily integrable into existing mainstream RL algorithms. Experimental results across multiple environments demonstrate that our approach improves RL efficiency, achieves superior performance, and holds promise as a fundamental technique in the field of reinforcement learning.

## 1 INTRODUCTION

Minimizing Bellman error is central to reinforcement learning (RL) algorithms Sutton & Barto (2018). RL optimizes decision-making by solving Markov Decision Processes (MDPs), with its underlying logic relying on the Bellman equation Bellman (1966). The Bellman equation defines how the state-action value function (Q-function) connects current decisions to long-term returns, making accurate estimation of the value function crucial. This process involves minimizing value estimation error Fujimoto et al. (2018), and its optimization directly impacts policy learning and improvement. Since the state-action value function serves as the foundation for policy optimization, effectively fitting Riedmiller (2005), approximating Sutton et al. (1999), updating Munos & Szepesvári (2008), and modeling Bellemare et al. (2017) it has become the core challenges in RL research.

Minimizing Bellman error is essentially minimizing value error Sutton (1988). Value error is defined based on the optimal state-value function and is generally not directly computable. When the value error reaches zero, it indicates that the value function has been perfectly fitted. With the advancement of neural networks, deep reinforcement learning has found increasingly broad applications, making the efficiency of value function fitting more critical. By improving the accuracy of Bellman error estimation Omura et al. (2024), optimizing the value function fitting process Patterson et al. (2022), and enhancing its efficiency, we can not only improve policy optimization but also increase the sample efficiency of RL algorithms.

The Bellman error serves as a proxy for the Value error Fujimoto et al. (2022). However, this proxy relationship does not guarantee equivalence between the two errors - it represents a trade-off. During optimization, the bias in the Bellman error is often ignored. When minimizing the Bellman error, the bias may change while the Value error remains constant. Due to both the linear nature of the Bellman equation and the way we evaluate Value error (using L2 or L1 norms), there can potentially exist multiple equivalent proxies for the same Value error (as illustrated with specific examples in Sec.4). Therefore, choosing an appropriate Bellman error and improving the value update process can help enhance the accuracy and efficiency of value function approximation.

054 Previous research has reshaped the Bellman error from the perspective of the reward function and  
 055 Q-value rather than addressing the inherent issues of the Bellman error itself. The reward function  
 056 and target Q-value are two crucial components of the Bellman Error. The Bellman Error can be re-  
 057 shaped by modifying the reward function, as demonstrated in various works on reward shaping Naik  
 058 et al. (2024), reward smoothing Schulman et al. (2015), reward scaling Haarnoja et al. (2018a;b)  
 059 and dense reward design Pathak et al. (2017); Osband et al. (2018); Burda et al. (2018). Research  
 060 focusing on target Q-values has primarily investigated methods to modify Q-value to promote di-  
 061 versity Van Seijen et al. (2017); Sun et al. (2022a) or stability Ioffe (2015); Gallici et al. (2024);  
 062 Fujimoto et al. (2024), as well as modeling their underlying distributions Bellemare et al. (2017);  
 063 Dabney et al. (2018); Hessel et al. (2018); Cetin & Celiktutan (2023).

064 In this paper, we investigate the origins of Bellman error bias and methods for its reduction. The  
 065 intuitive idea is to use **Monotonically** increasing linear **reward transformation** that preserve the  
 066 optimal policy while linearly reducing the bias in Bellman error through the transformed rewards.  
 067 We name this method MRT (Monotonic Reward Transformation). In terms of implementation, MRT  
 068 maintains two parallel Bellman iteration processes: one with default settings to predict Bellman  
 069 error bias, and another that incorporates the predicted bias as reward compensation into the target  
 070 Q-values, enabling low-bias Q-value updates. These low-bias Q-values are then used to guide policy  
 071 optimization. Notably, our method is plug-and-play, offering broad applicability across different  
 072 settings. We apply the MRT method to several mainstream algorithms, and experiments across  
 073 multiple environments demonstrate that MRT significantly improves sample efficiency and boosts  
 074 algorithm performance.

## 075 2 RELATED WORK

076 Reward signal plays a critical role in determining the success or failure of the RL algorithm. Reward  
 077 shaping (RS) has been extensively discussed in previous research, we introduce "Value Shaping"  
 078 (VS), which shares a strong connection with reward shaping through the Bellman Equation and is  
 079 similarly built upon the concept of preserving the optimal policy.

080 **Reward shaping** In general, any method that modifies the reward signal in RL can be consid-  
 081 ered a form of reward shaping. The concept of reward shaping was first introduced in (Ng et al.,  
 082 1999), which utilizes reward information to distinguish between states, enabling better policy learn-  
 083 ing while emphasizing that the optimal policy remains unchanged. In contrast, in sparse reward  
 084 environments, additional intrinsic rewards are often designed (Chentanez et al., 2004) to achieve  
 085 a similar goal. For instance, methods like RND (Pathak et al., 2017; Osband et al., 2018; Burda  
 086 et al., 2018) add reward signals based on prior knowledge, allowing the policy to learn more effec-  
 087 tively. Other works modify the way prior knowledge is utilized (Hu et al., 2020; Chen et al., 2022)  
 088 to achieve improved performance. Some studies also focus on policy optimization by altering the  
 089 reward signal to reduce the variance of the gradient, such as in GAE (Schulman et al., 2015).

090 **Value shaping** also includes multiple research area as value is updated based on Bellman equation,  
 091 some related to Bellman error reduction Kumar et al. (2019),and chain effect reduction Tang &  
 092 Berseth (2024).Some related to represent learning, such as Dueling networkWang et al. (2016),  
 093 BatchNorm Ioffe (2015); Bhatt et al. (2019),Spectral Normalization Bjorck et al. (2021) designed  
 094 for value normalization, LayerNorm Network Gallici et al. (2024); Fujimoto et al. (2024). Some  
 095 related to modeling related distribution, such as reward distribution Van Seijen et al. (2017); Sun  
 096 et al. (2022b), value distribution Bellemare et al. (2017); Hessel et al. (2018), which leads to a  
 097 series of research about distributional reinforcement learning, such as value decomposition Rashid  
 098 et al. (2020), value quantile regression Dabney et al. (2018). While some work make a progress  
 099 on variance reduction, such as reward Centering Naik et al. (2024) for value variance reduction,  
 100 Advantage baseline Mnih (2016) for policy gradient variance reduction. There are also many works  
 101 that utilize value shaping, such as reward scaling in the SAC Haarnoja et al. (2018a;b) paper.

108 

### 3 BACKGROUND

109 

#### 3.1 DEEP REINFORCEMENT LEARNING

110 Reinforcement learning (RL) is an optimization framework for tasks of a sequential nature (Sutton  
 111 & Barto, 2018). Typically, tasks are defined as a Markov decision process (MDP)  $(\mathcal{S}, \mathcal{A}, r, p,$   
 112  $d_0, \gamma)$ , where  $\mathcal{S}$  is a finite state space,  $\mathcal{A}$  is a finite action space,  $r : \mathcal{S} \times \mathcal{A} \rightarrow \mathbb{R}$  is a bounded  
 113 reward function (i.e.,  $|r(s, a)| \leq R_{\max}$  for some  $R_{\max} < \infty$ ),  $p(\cdot | s, a)$  denotes the transition  
 114 probability distribution over next states given  $(s, a)$ ,  $d_0$  is the initial state distribution, and  $\gamma \in [0, 1)$   
 115 is the discount factor. Actions are selected according to a policy  $\pi$ . The performance of a policy is  
 116 measured by its discounted return  
 117

$$118 J_r(\pi) = \mathbb{E}_\pi \left[ \sum_t^\infty \gamma^t r(s_t, a_t) \right]. \quad (1)$$

119 In reinforcement learning, the Bellman equations Bellman (1966) describe the relationship between  
 120 the value of a state (or state-action pair) and the expected return from that state onward. Below is  
 121 the expected Bellman operator  $\mathcal{T}$ .  
 122

$$123 \mathcal{T}Q^\pi(s, a) = \mathbb{E}_{s' \sim p, a' \sim \pi} [r(s, a) + \gamma Q^\pi(s', a')], \quad (2)$$

124 which relates the value of the current state-action pair to an expectation over the next state-action  
 125 pair. Given an approximate value function  $Q$  (distinguished from the true value function  $Q^\pi$  by  
 126 dropping the  $\pi$  superscript) of a target policy  $\pi$ , we denote the **Bellman error**  $\epsilon(s, a)$ :  
 127

$$128 \epsilon_Q(s, a) := Q(s, a) - \mathbb{E}_{s' \sim p, a' \sim \pi} [r(s, a) + \gamma Q(s', a')]. \quad (3)$$

129 In practice, the Bellman error is approximated by **Temporal Difference** (TD) Sutton (1988) **error**  
 130  $\delta(i)$ , for a transition  $i := (s, a, r, s')$ , the TD error is,  
 131

$$132 \delta_Q(i) := Q(s, a) - (r(s, a) + \gamma Q(s', a')),$$

133 where  $a' \sim \pi$ . The relationship between the TD error and the Bellman error can be described as  
 134 follows:  
 135

$$\epsilon_Q(s, a) = \mathbb{E}_{s', a'} [\delta_Q(i)].$$

136 In policy evaluation, the main objective of interest is a loss (such as the MSE or L1) over the **value**  
 137 **error**  $\Delta_Q(s, a)$ , the distance of an approximate value function  $Q$  to the true value function  $Q^\pi$  of  
 138 the target policy  $\pi$ :  
 139

$$140 \Delta_Q(s, a) := Q(s, a) - Q^\pi(s, a). \quad (4)$$

141 Value error is often unmeasurable, as the true value function  $Q^\pi$  is unobtainable without the un-  
 142 derlying MDP. While both the Bellman error and the value error are defined with respect to  $Q$ , for  
 143 simplicity we drop the subscript when the error terms are not in reference to a specific value func-  
 144 tion. The relationship between the Bellman error and the value error has been explored in prior  
 145 work Fujimoto et al. (2022), and it is formalized in the following:  
 146

147 **Proposition 3.1** (Value error as a function of Bellman error). *For any state-action pair  $(s, a) \in$   
 148  $\mathcal{S} \times \mathcal{A}$ , with state action distribution  $d^\pi(s', a' | s, a) = \frac{1}{1-\gamma} \sum_{t=0}^\infty \gamma^t p^\pi((s, a) \rightarrow s', t) \pi(a' | s')$ , the  
 149 value error  $\Delta_Q(s, a)$  can be defined as a function of the Bellman error  $\epsilon_Q$*

$$150 \Delta_Q(s, a) = \frac{1}{1-\gamma} \mathbb{E}_{(s', a') \sim d^\pi(\cdot | s, a)} [\epsilon_Q(s', a')]. \quad (5)$$

151 This proposition explains the relationship between value error and Bellman error from the perspec-  
 152 tive of the state distribution.  
 153

154 

#### 3.2 LINEAR REWARD TRANSFORMATION

155 In a Markov Decision Process (MDP), a linear transformation of the reward function generally does  
 156 not affect the optimal policy, depending on the specific form of the linear transformation.  
 157

162 Suppose the transformed reward function is given by  
 163

$$164 \quad r'(s, a) = \alpha \cdot r(s, a) + \beta$$

165 where  $\alpha$  and  $\beta$  are constants, with  $\alpha > 0$ . a linear transformation of the form  $r'(s, a) = \alpha \cdot r(s, a) + \beta$   
 166 with  $\alpha > 0$  will not affect the choice of the optimal policy. However, if  $\alpha < 0$  (i.e., the transfor-  
 167 mation involves a negative scaling factor), it will reverse the reward priorities, causing originally higher  
 168 rewards to become lower, which would affect the optimal policy. Therefore, maintaining  $\alpha > 0$  is  
 169 essential. We also refer to linear transformations with  $\alpha > 0$  as MRT(Monotonic increasing linear  
 170 Reward Transformation). This name provides better understanding and intuition.  
 171

## 172 4 MITIGATING THE BIAS OF BELLMAN ERROR

173 By appropriately altering the shape of the target domain, we can make the Q-function easier to learn.  
 174 This means that we should pay attention to the shape of Bellman error. In the following content, to  
 175 simplify expressions, the inputs of functions will be omitted when it's unnecessary. For example,  
 176 the state-value function  $Q(s, a)$  will be written as  $Q$ , the reward function  $r(s, a)$  will be written as  
 177  $r$ , and the bias function  $b(s, a)$  will be written as  $b$ .  
 178

179 **Problem statement.** The Bellman equation provides a recursive and iterative framework for value  
 180 learning, offering a method to estimate long-term returns. However, when function approximation  
 181 and temporal difference learning are introduced, any bias introduced during the value update not  
 182 only persists but also propagates throughout the iterative process Fujimoto et al. (2022); Farahmand  
 183 et al. (2010). This is because both value error and Bellman error are evaluated based on the relative  
 184 absolute difference between two target values.  
 185

186 Although this bias may not necessarily prevent the optimal policy from converging, it can signifi-  
 187 cantly influence the learning process of the value function. To illustrate this phenomenon, we borrow  
 188 an example Fujimoto et al. (2022) that demonstrates the existence of such bias.

189 **Remark 4.1 (Bellman error hides bias).** Let  $Q^\pi$  be the true value function for some MDP and  
 190 policy  $\pi$ . We define the following approximate value functions:

$$191 \quad Q_1 = Q^\pi + 1 \quad (\text{bias is correlated}),$$

$$192 \quad Q_2 = Q^\pi \pm 1 \quad (\text{bias is uncorrelated}),$$

193 where  $\pm 1$  denotes a random operator, taking the value  $+1$  or  $-1$  with equal probability. In both  
 194 cases, following Eq. 4, the value error, measured by MSE or L1 loss will be 1 for any state-action  
 195 pair. Following Eq. 2, expanding the expectation of next Q-value, the Bellman error of  $Q_1$  will be  
 196  $1 - \gamma \mathbb{E}[1] = 1 - \gamma$ , while the Bellman error of  $Q_2$  will be  $|\pm 1 - \gamma \mathbb{E}[\pm 1]| = 1$ . This means that  
 197 when using Bellman error to estimate value error, measured with MSE or L1 loss, there exists bias  
 198 in Bellman error.  
 199

200 **Remark 4.2 (Bellman iteration propagates bias).** Due to the fact that Bellman iteration updates  
 201 and unfolds through bootstrapping, the biases introduced during this process cannot be eliminated by  
 202 its own mechanism. Instead, these biases accumulate and propagate throughout the iterations Farah-  
 203 mand et al. (2010). The formal statement is as follows (omitting the reward function):  
 204

$$204 \quad \mathcal{T}Q' = Q' + 1 \quad (\text{next time step Q-value}),$$

$$205 \quad \mathcal{T}Q = Q + 1 \quad (\text{current time step Q-value}),$$

$$206 \quad Q = \mathbb{E}[Q' + 1] + 1 \quad (\text{bias is accumulated}).$$

207 It can be seen that bias accumulates during the Bellman iteration. Bias can be introduced in various  
 208 forms, and our main concern is how to eliminate or reduce its impact on value learning. Next, we  
 209 discuss the sources of bias and explore methods to mitigate it.  
 210

### 212 4.1 ORIGINS OF BIAS AND REWARD COMPENSATION

213 From the previous discussion, it is clear that irrelevant biases cannot be controlled. If they follow  
 214 a normal distribution, they also seem not to affect the estimation of values. Therefore, our focus  
 215 should be on relevant biases, particularly those that are dependent on the state and action.

216 Regarding biases that depend on the state and action, we can draw the following conclusions:  
 217

218 **Proposition 4.3** (Bias arises from accumulated Bellman errors.). *For any state-action pair*  
 219  *$(s_0, a_0) \in \mathcal{S} \times \mathcal{A}$ , the value error  $\Delta_Q(s_0, a_0)$  is the accumulation of the Bellman errors  $\epsilon_Q$  over*  
 220 *future time steps:*

$$221 \quad \Delta_Q(s_0, a_0) = \epsilon_Q(s_0, a_0) + \mathbb{E}_\pi \left[ \sum_{t=1}^{\infty} \gamma^t \epsilon_Q(s_t, a_t) \right]. \quad (6)$$

224 This proposition explains the relationship between value error and Bellman error from the perspective  
 225 of trajectory interaction. When minimizing the value error, we focus on the Bellman error but  
 226 neglect the Bellman errors from the remaining interactions, which are the primary sources of bias.

227 Due to the linear nature of the Bellman operator, there exists a complementary relationship between  
 228 the reward and the bias of the Bellman error. To account for more general cases, we do not assume  
 229 that  $\mathbb{E}_\pi [\sum_{t=1}^{\infty} \gamma^t \epsilon(s_t, a_t)]$  is known. Instead, the more general assumption is as follows:

230 **Assumption 4.4.** We assume that  $\epsilon_Q$  contains some unpredictable bias  $b$ . The ideal Bellman error  
 231 can then be expressed as:

$$232 \quad \epsilon_Q^* = \epsilon_Q - b \quad (7)$$

234 Previous work focused on minimizing  $\epsilon_Q$  rather than minimizing  $\epsilon_Q^*$ , which could result in optimization  
 235 operations that do not actually reduce  $\epsilon_Q^*$ . Instead, this may cause the individual bias to keep  
 236 changing, even though the expectation of the bias does not necessarily change. It is additionally  
 237 noteworthy that  $\epsilon_Q^* = \Delta_Q$ . Based on two key observations: the Bellman expectation equation is  
 238 linear, and a linear transformation of the reward function does not affect policy convergence, it can  
 239 be inferred that the bias in the Bellman error can be compensated for by modifying the reward. We  
 240 know that the reward can be linearly transformed without affecting the convergence of the optimal  
 241 policy:

$$242 \quad r' = \alpha \cdot r + \beta$$

243 Therefore, we can replace the reward function of  $r$  to  $r'$ , and perform the following transformation  
 244 on the Bellman error:

$$245 \quad \epsilon_Q' = \epsilon_Q + r - r' \quad (8)$$

246 This essentially implies that  $r - r'$  can serve as a compensation term to balance the bias as much as  
 247 possible, thereby simplifying the fitting of the Q-value. And in practice, we can adjust the parameter  
 248 of  $\alpha$  to make the  $r - r'$  be close to  $-b$ , such we can have better proxy error  $\epsilon_Q'$  for the value error to  
 249 fitting the Q-function. Intuitively, at a certain stage of the learning process, when the Bellman error  
 250 is fixed, our additional objective is to minimize both the Bellman error and the bias. For example:

$$253 \quad \min_{r'} |\epsilon_Q' - \epsilon_Q^*| = \min_{r'} | -b - r + r' | \quad (9)$$

255 The issue here is that we cannot possibly know what the expected bias  $b$  actually is.

## 257 4.2 MINIMIZE THE TRANSFORMED BELLMAN ERROR

259 Actually, there's a trade-off that could potentially help address this. Specifically, we can minimize  
 260 the following:

$$262 \quad \min_{r'} \|\epsilon_Q' - \epsilon_Q^*\| \leq \min_{r'} \epsilon_Q' + \min_{r'} |\epsilon_Q^*| \quad (10)$$

264 Eq. 10 shows that the optimal  $\epsilon_Q^*$  no longer requires optimization and is independent of  $r'$ , so it  
 265 can be omitted. As a result, we obtain a very concise objective function, what we need to do is  
 266 transform reward function to minimize  $\epsilon_Q'$ . This (Eq. 8) transformed Bellman error can be regarded  
 267 as a better proxy for value error minimization than naive Bellman error. Eq. 10 leads to  $\epsilon_Q' =$   
 268  $|\epsilon_Q^*|$  or  $\epsilon_Q^*$ . Since we do not know the sign of  $\epsilon_Q^*$ , and the Q-value is typically reported to be  
 269 overestimated Fujimoto et al. (2018), we consider this relaxation (Eq. 10) acceptable by minimizing  
 this objective periodically.

Now let's bring the problem back into the framework of reinforcement learning. Let's rethink the effect of the reward transformation, to derive some practice idea. Refer to Eq. 1, maximizing the sum of transformed rewards does guarantee a policy that also maximizes original rewards:

$$\arg \max_{\pi \in \Pi} J_{r'}(\pi) = \arg \max_{\pi \in \Pi} J_r(\pi).$$

In this formula,  $r'$  is not fixed. Constantly changing  $r'$  implies that collecting trajectories under different reward scales will result in data with varying reward scales. Training with data from different scales is almost impossible. Next, we will provide a solution to this problem, and explain why our method is value shaping rather than reward shaping.

#### 4.3 VALUE SHAPING IS ALL YOU NEED

The reward shaping method evaluates the agent's performance based on the reshaped reward. If we consider our MRT method as a reward shaping approach, the resulting optimization objective is:

$$\begin{aligned} & \max_{\pi' \in \Pi} J_{r'}(\pi') \\ \text{subject to } & J_r(\pi') - \max_{\pi} J_r(\pi) = 0 \\ & r' = \arg \min \mathbb{E}[\epsilon'_Q]^2. \end{aligned}$$

Here, we consider minimizing all Bellman errors, so we use the MSE loss. It is worth noting that some reward shaping methods do not satisfy the second constraint and instead heuristically modify the reward signal. Based on the fact that our purpose in modifying the reward is not to enhance the reward function in a specific aspect, our objective can therefore simply be:

$$\begin{aligned} & \max_{\pi \in \Pi} J_r(\pi) \\ \text{subject to } & J_{r'}(\pi) - \max_{\pi'} J_{r'}(\pi') = 0 \\ & r' = \arg \min \mathbb{E}[\epsilon'_Q]^2. \end{aligned} \tag{11}$$

Solving this optimization problem can be understood as proposing a policy  $\pi'$  that maximizes  $J_{r'}$  and then verifying whether the proposed  $r'$  is feasible by improving the accuracy of the Bellman error. Referring to Eq. 9, we know that the optimal reward modification is given by  $r'(s, a) = r(s, a) + b(s, a)$ . This implies that we do not need to know the exact form of  $r$ . If we can accurately estimate  $b$ , then by using  $\hat{r}' = r + \hat{b}$ , we can complete the closed-loop implementation of our method. Although  $b$  is unknown, we can reasonably infer that if we maintain an estimate  $\hat{b}$ , it should be as close as possible to  $\epsilon_Q$  to minimize Eq. 7. Referring to Eq. 6, we know that the bias is related to the accumulated Bellman error. Referring to Eq. 11, the argmin of the sampled Bellman error is the expectation of the Bellman error, which implies that  $\hat{b} = -\mathbb{E}[\epsilon_Q]$ .

In practice, we initialize two value-learning processes. One follows the standard setting and is used to estimate the bias in the Bellman error, while the other, referred to as the lower-bias  $Q$ , is designed to learn a value function with reduced bias. By maintaining these two independent value-learning processes, our approach simultaneously mitigates value estimation errors and prevents error propagation. Referring to Eq. 2, we first initialize a standard Bellman iteration:

$$\mathcal{T}Q_1(s, a) = \mathbb{E}_{r, s' \sim p, a' \sim \pi} [r + \gamma Q_1(s', a')]. \tag{12}$$

The function  $Q_1$  is updated to minimize the difference between  $Q_1$  and  $\mathcal{T}Q_1$ . This process allows us to estimate the bias, denoted as  $\hat{b}$ , which is then used as the target for  $Q_2$ :

$$Q'_1(s, a) = \mathbb{E}_{r, s' \sim p, a' \sim \pi} [r + \hat{b} + \gamma Q_1(s', a')]. \tag{13}$$

The function  $Q_2$  is then updated to minimize the difference between  $Q_2$  and the low-bias target  $Q'_1$ . Following the delayed update trick Fujimoto et al. (2018), our framework periodically assigns  $Q_2$  to  $Q_1$  to achieve a low-variance Q-value update. Our method is considered a **value shaping** approach because the target Q-values are explicitly modified. Compared to reward centering Naik et al. (2024), our approach instead centers the Bellman error.

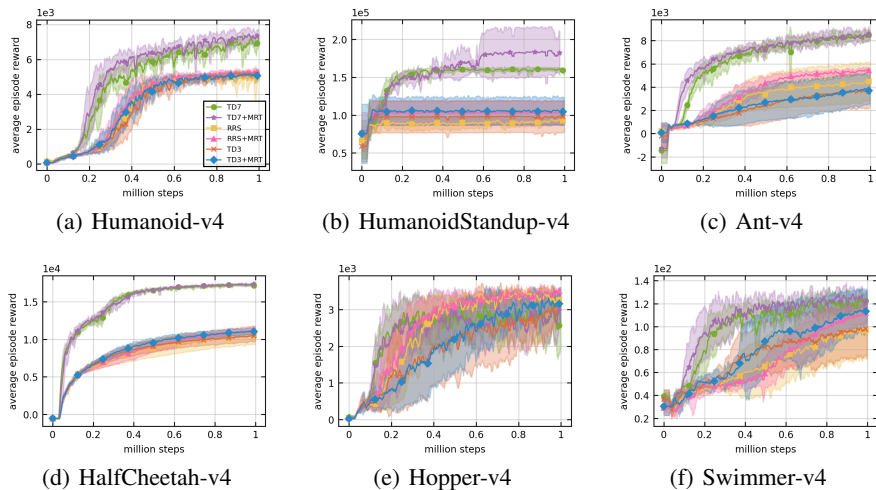
324 **5 EXPERIMENTS**  
 325

326 We conducted experiments on six continuous control tasks using the Mujoco Todorov et al. (2012)  
 327 platform. The environments range from simple to complex, specifically: Swimmer-v4, Hopper-v4,  
 328 HalfCheetah-v4, Ant-v4, HumanoidStandup-v4, and Humanoid-v4. The experiments were run on  
 329 a hardware platform consisting of four Intel Gold 6230 CPUs and four RTX 3090 GPUs. Each  
 330 algorithm was executed six times using random seeds from 1 to 6. Evaluated with 1M time steps,  
 331 TD3 consumes 63.5 minutes, while TD3+MRT consumes 72.1 minutes. Practical algorithm and  
 332 hyper-parameters are in the appendix( see Algorithm 1 and Table 2).

333 We compared three of the most well-known baseline algorithms in deep reinforcement learning,  
 334 each of which has had a significant impact on the field. TD3 Fujimoto et al. (2018) mitigates the  
 335 overestimation of predicted values and stabilizes the value function update process. RRS Sun et al.  
 336 (2022a) shifts the reward, leading to a different initialization of the Q-function, which enhances  
 337 performance by avoiding suboptimal solutions through diverse exploration. TD7 Fujimoto et al.  
 338 (2024) modifies the neural network architecture and the inputs to the Q-function, achieving the  
 339 strongest empirical performance.

340 **5.1 THE IMPACT OF BIAS REDUCTION ON POLICY OPTIMIZATION**  
 341

342 We first consider the impact of bias reduction on policy optimization. Ideally, bias reduction can  
 343 improve the accuracy of the Q-function, thereby having a positive effect on policy optimization.  
 344 The purpose of bias reduction is also to accelerate policy optimization during the learning process.  
 345 An inaccurate Q-function leads to inaccurate policy gradients. Therefore, evaluating the impact of  
 346 bias reduction from the perspective of policy optimization can indirectly reflect its effectiveness.  
 347 Based on this, we assess the effect of MRT on the three baseline algorithms. The results are shown  
 348 in Fig. 1.



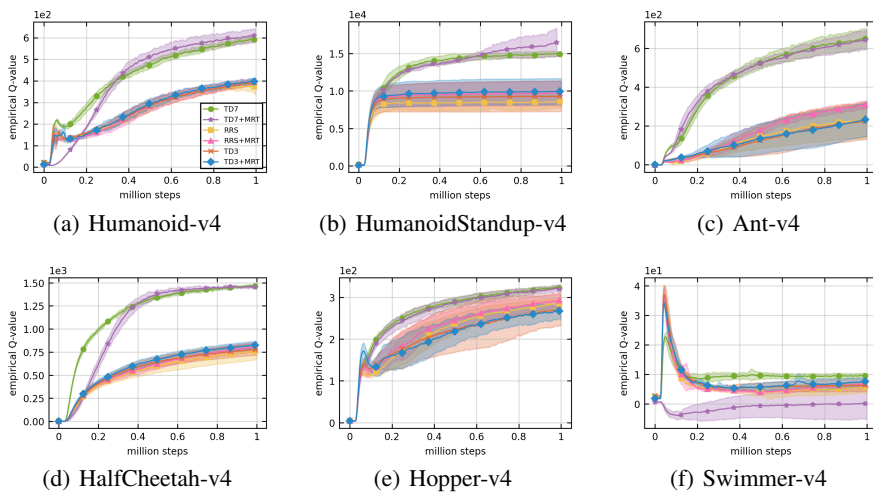
367 Figure 1: Learning curves of all algorithms. The x-axis represents time steps, with one million  
 368 interaction steps, and the y-axis represents the average episode return.

369 From the results shown in the figure, we can observe that in more complex environments, such as  
 370 those involving the control of two humanoid robots (Fig. 1(a-b)), MRT demonstrates a significant  
 371 advantage. By providing more accurate Q-value estimations, MRT enhances the efficiency of policy  
 372 optimization. It not only improves the sample efficiency of TD7 but also outperforms both RRS  
 373 and TD3. In the Humanoid-v4 environment, MRT enhances the final convergence performance of  
 374 the original algorithm. In the Ant-v4 environment, MRT provides noticeable benefits to the base-  
 375 line algorithms in the early stages of training. However, in the HalfCheetah-v4 environment, the  
 376 difference is less pronounced. Since this environment has the second-largest reward scale (with  
 377 HumanoidStandup-v4 being the largest), the stability of the algorithm may play a role in this ob-  
 378 servation. Indeed, in both of these environments, the learning process appears relatively stable. In

378 the Hopper-v4 environment, the TD7 algorithm, which incorporates LayerNorm, does not seem to  
 379 handle the task well. MRT does not significantly improve TD7’s performance in this case but instead  
 380 provides more noticeable benefits to the RRS algorithm, especially in the early training phase. Fi-  
 381 nally, in the Swimmer-v4 environment, MRT enhances learning accuracy by reducing bias, leading  
 382 to improved sample efficiency across all three algorithms.  
 383

## 384 5.2 THE IMPACT OF BIAS REDUCTION ON VALUE UPDATE

386 After verifying the impact of reducing Bellman error bias on policy optimization, the next focus is  
 387 on its effect on value updates. The value function heavily depends on the magnitude and accuracy  
 388 of the Bellman error. While bias reduction has an indirect impact on policy optimization, it directly  
 389 influences value updates. Since Q-function optimization is achieved by minimizing the Bellman  
 390 error, the two are closely related. Analyzing Q-value trends provides insights into the entire training  
 391 process. Therefore, we recorded the estimated Q-values based on the sampled transitions during  
 392 training. Typically, as the policy improves, the Q-value increases accordingly. However, different al-  
 393 gorithms affect the Q-value update process differently, reflecting their influence on value estimation.  
 394 The evaluation results of the Q-values are shown in Figure 2.



412 Figure 2: Empirical Q-value of all algorithms. The x-axis represents time steps, with one million  
 413 interaction steps, and the y-axis represents the estimated empirical Q-value over the sampled transi-  
 414 tions.

415 From Figure 2, we can observe that, compared to baseline algorithms, the Q-values in the early  
 416 training phase are generally lower when using the MRT algorithm. This is evident in environments  
 417 such as Humanoid-v4, HumanoidStandup-v4, HalfCheetah-v4, and Swimmer-v4. The reason for  
 418 this is that MRT reduces the original Bellman error, leading to smaller update magnitudes, which in  
 419 some cases also results in higher accuracy. In the later training stages, if previous algorithms were  
 420 limited by Q-value accuracy issues, our method’s Q-values tend to catch up and even surpass them  
 421 over time.

422 Another noteworthy observation is that, unlike policy evaluation results, Q-value updates are rel-  
 423 atively stable. Although the collected samples represent only a subset of all possible transitions,  
 424 Q-values generally continue to grow in most environments. However, in the Swimmer-v4 environ-  
 425 ment, due to the TD7 algorithm using priority sampling based on TD error and our method reducing  
 426 the error magnitude, the Q-value update curve appears less consistent.

## 428 5.3 THE IMPACT OF BIAS REDUCTION ON BELLMAN ERROR

430 Besides the two previously mentioned metrics, the most important one we should focus on is the  
 431 change in Bellman error, as our entire paper revolves around discussing it. This metric typically re-  
 flects the smoothness of the learning process, where a smaller Bellman error indicates convergence.

At the same time, a larger Bellman error suggests greater prediction errors, which can lead to instability. However, on the other hand, a larger Bellman error also implies a greater optimization step. Since it can serve both as an optimization objective and an evaluation metric, Bellman error has a dual nature. We aim to compare the average Bellman error across different algorithms to assess the potential impact of Bias Reduction on the results. The variation in Bellman error during the experiments is recorded in Fig. 3.

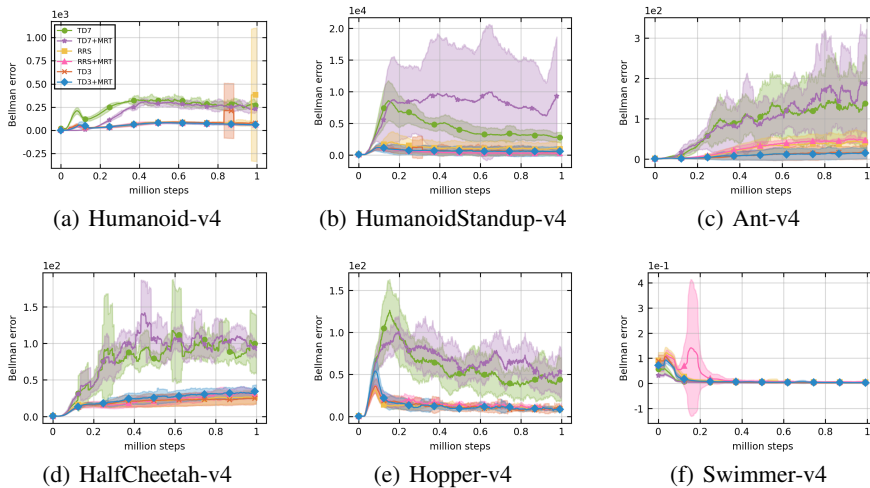


Figure 3: Empirical estimated square Bellman error of all algorithms. The x-axis represents time steps, with one million interaction steps, and the y-axis represents the average estimated square Bellman error over the sampled transitions.

Observing Fig. 3, we find that in the Humanoid-v4 environment, the MRT algorithm effectively avoids the late-stage anomalies in Bellman error compared to TD3 and RRS, while making the optimization process more stable when compared to TD7. In the HumanoidStandup-v4 environment, as the algorithms are still improving, our results have not yet fully converged. However, our method demonstrates greater stability compared to the RRS algorithm. Similarly, in the Ant-v4 environment, the MRT algorithm consistently exhibits a larger Bellman error than the TD7 algorithm. This is because TD7 employs priority sampling based on TD error and clips small TD errors, a technique that does not benefit our algorithm. Similar trends can be observed in the HalfCheetah-v4 and Hopper-v4 environments. Since both RRS and TD3 use random sampling, the comparison between RRS and TD3 is more convincing. In the Swimmer-v4 environment, the RRS+MRT algorithm shows a noticeable spike in Bellman error, because that a larger Bellman error results in larger step sizes, making it more effective in environments requiring exploration.

## 6 CONCLUSION

This paper investigates the reduction of Bellman error bias through linear reward transformation. By leveraging the fact that linear reward transformations do not affect policy convergence, we estimate the bias in the Bellman error and incorporate it into the reward function to influence the value update process. This process is carried out using two parallel Bellman iterations, where bias estimation techniques and linear reward transformation are employed. This simplifies the MRT algorithm, making it applicable to any deep reinforcement learning algorithm. Experimental results show that reducing Bellman error bias improves sample efficiency. Given the critical role of Bellman error in reinforcement learning, there is significant potential for further research. Future work will focus on developing more advanced techniques for bias prediction and reduction.

486  
487  
ETHICS STATEMENT488  
489  
490  
491  
492  
493  
494  
495  
496  
497  
498  
499  
This research did not involve human participants, personal data, or animals, and therefore did not re-  
quire institutional ethics approval. All experiments were conducted using publicly available datasets  
and simulated environments, ensuring that no privacy or safety concerns arise.500  
501  
502  
503  
504  
505  
506  
507  
508  
509  
510  
511  
512  
513  
514  
515  
516  
517  
518  
519  
520  
521  
522  
523  
524  
525  
526  
527  
528  
529  
530  
531  
532  
533  
534  
535  
536  
537  
538  
539  
REPRODUCIBILITY STATEMENT500  
501  
502  
503  
504  
505  
506  
507  
508  
509  
510  
511  
512  
513  
514  
515  
516  
517  
518  
519  
520  
521  
522  
523  
524  
525  
526  
527  
528  
529  
530  
531  
532  
533  
534  
535  
536  
537  
538  
539  
We provide the implementation code and configuration files in the supplementary material. All  
reported results are averaged over six random seeds (1, 2, 3, 4, 5, 6). Shaded regions in the figures  
denote one standard deviation around the mean. Details of the hardware platform and computational  
time are presented at the beginning of the Experiments section.500  
501  
502  
503  
504  
505  
506  
507  
508  
509  
510  
511  
512  
513  
514  
515  
516  
517  
518  
519  
520  
521  
522  
523  
524  
525  
526  
527  
528  
529  
530  
531  
532  
533  
534  
535  
536  
537  
538  
539  
REFERENCES500  
501  
502  
503  
504  
505  
506  
507  
508  
509  
510  
511  
512  
513  
514  
515  
516  
517  
518  
519  
520  
521  
522  
523  
524  
525  
526  
527  
528  
529  
530  
531  
532  
533  
534  
535  
536  
537  
538  
539  
Marc G Bellemare, Will Dabney, and Rémi Munos. A distributional perspective on reinforcement  
learning. In *International conference on machine learning*, pp. 449–458. PMLR, 2017.  
Richard Bellman. Dynamic programming. *science*, 153(3731):34–37, 1966.  
Aditya Bhatt, Daniel Palenicek, Boris Belousov, Max Argus, Artemij Amiranashvili, Thomas Brox,  
and Jan Peters. Crossq: Batch normalization in deep reinforcement learning for greater sample  
efficiency and simplicity. *arXiv preprint arXiv:1902.05605*, 2019.  
Nils Bjorck, Carla P Gomes, and Kilian Q Weinberger. Towards deeper deep reinforcement learning  
with spectral normalization. *Advances in neural information processing systems*, 34:8242–8255,  
2021.  
Yuri Burda, Harrison Edwards, Amos Storkey, and Oleg Klimov. Exploration by random network  
distillation. *arXiv preprint arXiv:1810.12894*, 2018.  
Edoardo Cetin and Oya Celiktutan. Learning pessimism for reinforcement learning. In *Proceedings  
of the AAAI conference on artificial intelligence*, volume 37, pp. 6971–6979, 2023.  
Eric Chen, Zhang-Wei Hong, Joni Pajarinen, and Pulkit Agrawal. Redeeming intrinsic rewards via  
constrained optimization. *Advances in Neural Information Processing Systems*, 35:4996–5008,  
2022.  
Nuttapong Chentanez, Andrew Barto, and Satinder Singh. Intrinsically motivated reinforcement  
learning. *Advances in neural information processing systems*, 17, 2004.  
Will Dabney, Mark Rowland, Marc Bellemare, and Rémi Munos. Distributional reinforcement  
learning with quantile regression. In *Proceedings of the AAAI conference on artificial intelligence*,  
volume 32, 2018.  
Amir-massoud Farahmand, Csaba Szepesvári, and Rémi Munos. Error propagation for approximate  
policy and value iteration. *Advances in neural information processing systems*, 23, 2010.  
Scott Fujimoto, Herke Hoof, and David Meger. Addressing function approximation error in actor-  
critic methods. In *International conference on machine learning*, pp. 1587–1596. PMLR, 2018.  
Scott Fujimoto, David Meger, Doina Precup, Ofir Nachum, and Shixiang Shane Gu. Why should  
i trust you, bellman? the bellman error is a poor replacement for value error. *arXiv preprint  
arXiv:2201.12417*, 2022.  
Scott Fujimoto, Wei-Di Chang, Edward Smith, Shixiang Shane Gu, Doina Precup, and David Meger.  
For sale: State-action representation learning for deep reinforcement learning. *Advances in Neural  
Information Processing Systems*, 36, 2024.  
Matteo Gallici, Mattie Fellows, Benjamin Ellis, Bartomeu Pou, Ivan Masmitja, Jakob Nicolaus  
Foerster, and Mario Martin. Simplifying deep temporal difference learning. *arXiv preprint  
arXiv:2407.04811*, 2024.

540 Tuomas Haarnoja, Aurick Zhou, Pieter Abbeel, and Sergey Levine. Soft actor-critic: Off-policy  
 541 maximum entropy deep reinforcement learning with a stochastic actor. In *International conference on machine learning*, pp. 1861–1870. PMLR, 2018a.  
 542

543 Tuomas Haarnoja, Aurick Zhou, Kristian Hartikainen, George Tucker, Sehoon Ha, Jie Tan, Vikash  
 544 Kumar, Henry Zhu, Abhishek Gupta, Pieter Abbeel, et al. Soft actor-critic algorithms and appli-  
 545 cations. *arXiv preprint arXiv:1812.05905*, 2018b.  
 546

547 Matteo Hessel, Joseph Modayil, Hado Van Hasselt, Tom Schaul, Georg Ostrovski, Will Dabney, Dan  
 548 Horgan, Bilal Piot, Mohammad Azar, and David Silver. Rainbow: Combining improvements in  
 549 deep reinforcement learning. In *Proceedings of the AAAI conference on artificial intelligence*,  
 550 volume 32, 2018.  
 551

552 Yujing Hu, Weixun Wang, Hangtian Jia, Yixiang Wang, Yingfeng Chen, Jianye Hao, Feng Wu, and  
 553 Changjie Fan. Learning to utilize shaping rewards: A new approach of reward shaping. *Advances  
 554 in Neural Information Processing Systems*, 33:15931–15941, 2020.  
 555

556 Sergey Ioffe. Batch normalization: Accelerating deep network training by reducing internal covari-  
 557 ate shift. *arXiv preprint arXiv:1502.03167*, 2015.  
 558

559 Sham Kakade and John Langford. Approximately optimal approximate reinforcement learning.  
 560 In *Proceedings of the Nineteenth International Conference on Machine Learning*, pp. 267–274,  
 2002.  
 561

562 Aviral Kumar, Justin Fu, Matthew Soh, George Tucker, and Sergey Levine. Stabilizing off-policy  
 563 q-learning via bootstrapping error reduction. *Advances in neural information processing systems*,  
 32, 2019.  
 564

565 Volodymyr Mnih. Asynchronous methods for deep reinforcement learning. *arXiv preprint  
 566 arXiv:1602.01783*, 2016.  
 567

568 Rémi Munos and Csaba Szepesvári. Finite-time bounds for fitted value iteration. *Journal of Machine  
 569 Learning Research*, 9(5), 2008.  
 570

571 Abhishek Naik, Yi Wan, Manan Tomar, and Richard S Sutton. Reward centering. *arXiv preprint  
 572 arXiv:2405.09999*, 2024.  
 573

574 Andrew Y Ng, Daishi Harada, and Stuart Russell. Policy invariance under reward transformations:  
 575 Theory and application to reward shaping. In *Icml*, volume 99, pp. 278–287, 1999.  
 576

577 Motoki Omura, Takayuki Osa, Yusuke Mukuta, and Tatsuya Harada. Symmetric q-learning: Re-  
 578 ducing skewness of bellman error in online reinforcement learning. In *Proceedings of the AAAI  
 Conference on Artificial Intelligence*, volume 23, pp. 14474–14481, 2024.  
 579

580 Ian Osband, John Aslanides, and Albin Cassirer. Randomized prior functions for deep reinforcement  
 581 learning. *Advances in Neural Information Processing Systems*, 31, 2018.  
 582

583 Deepak Pathak, Pulkit Agrawal, Alexei A Efros, and Trevor Darrell. Curiosity-driven exploration  
 584 by self-supervised prediction. In *International conference on machine learning*, pp. 2778–2787.  
 585 PMLR, 2017.  
 586

587 Andrew Patterson, Adam White, and Martha White. A generalized projected bellman error for off-  
 588 policy value estimation in reinforcement learning. *Journal of Machine Learning Research*, 23  
 589 (145):1–61, 2022.  
 590

591 James Queeney, Yannis Paschalidis, and Christos G Cassandras. Generalized proximal policy op-  
 592 timization with sample reuse. *Advances in Neural Information Processing Systems*, 34:11909–  
 593 11919, 2021.  
 594

595 Tabish Rashid, Mikayel Samvelyan, Christian Schroeder De Witt, Gregory Farquhar, Jakob Foerster,  
 596 and Shimon Whiteson. Monotonic value function factorisation for deep multi-agent reinforce-  
 597 ment learning. *Journal of Machine Learning Research*, 21(178):1–51, 2020.  
 598

594 Martin Riedmiller. Neural fitted q iteration–first experiences with a data efficient neural reinforce-  
 595 ment learning method. In *Machine learning: ECML 2005: 16th European conference on machine*  
 596 *learning, Porto, Portugal, October 3-7, 2005. proceedings 16*, pp. 317–328. Springer, 2005.

597

598 John Schulman. Trust region policy optimization. *arXiv preprint arXiv:1502.05477*, 2015.

599 John Schulman, Philipp Moritz, Sergey Levine, Michael Jordan, and Pieter Abbeel. High-  
 600 dimensional continuous control using generalized advantage estimation. *arXiv preprint*  
 601 *arXiv:1506.02438*, 2015.

602

603 Hao Sun, Lei Han, Rui Yang, Xiaoteng Ma, Jian Guo, and Bolei Zhou. Exploit reward shifting  
 604 in value-based deep-rl: Optimistic curiosity-based exploration and conservative exploitation via  
 605 linear reward shaping. In S. Koyejo, S. Mohamed, A. Agarwal, D. Belgrave, K. Cho, and A. Oh  
 606 (eds.), *Advances in Neural Information Processing Systems*, volume 35, pp. 37719–37734. Curran  
 607 Associates, Inc., 2022a.

608 Hao Sun, Lei Han, Rui Yang, Xiaoteng Ma, Jian Guo, and Bolei Zhou. Exploit reward shifting  
 609 in value-based deep-rl: Optimistic curiosity-based exploration and conservative exploitation via  
 610 linear reward shaping. *Advances in neural information processing systems*, 35:37719–37734,  
 611 2022b.

612 Richard S Sutton. Learning to predict by the methods of temporal differences. *Machine learning*,  
 613 3:9–44, 1988.

614

615 Richard S Sutton and Andrew G Barto. *Reinforcement learning: An introduction*. MIT press, 2018.

616 Richard S Sutton, David McAllester, Satinder Singh, and Yishay Mansour. Policy gradient meth-  
 617 ods for reinforcement learning with function approximation. *Advances in neural information*  
 618 *processing systems*, 12, 1999.

619

620 Hongyao Tang and Glen Berseth. Improving deep reinforcement learning by reducing the chain  
 621 effect of value and policy churn. *arXiv preprint arXiv:2409.04792*, 2024.

622 Emanuel Todorov, Tom Erez, and Yuval Tassa. Mujoco: A physics engine for model-based control.  
 623 In *2012 IEEE/RSJ international conference on intelligent robots and systems*, pp. 5026–5033.  
 624 IEEE, 2012.

625

626 Harm Van Seijen, Mehdi Fatemi, Joshua Romoff, Romain Laroche, Tavian Barnes, and Jeffrey  
 627 Tsang. Hybrid reward architecture for reinforcement learning. *Advances in Neural Information*  
 628 *Processing Systems*, 30, 2017.

629 Ziyu Wang, Tom Schaul, Matteo Hessel, Hado Hasselt, Marc Lanctot, and Nando Freitas. Dueling  
 630 network architectures for deep reinforcement learning. In *International conference on machine*  
 631 *learning*, pp. 1995–2003. PMLR, 2016.

632

633

634

635

636

637

638

639

640

641

642

643

644

645

646

647

648 **A PROOF**  
 649

650 In the proof section, for better readability, we have simplified some expressions. For example, we  
 651 use  $\Delta$  to represent  $\Delta_Q$ .  
 652

653 **A.1 PROOF OF PROPOSITION 3.1**  
 654

655 **Proposition 3.1 (Value error as a function of Bellman error).** *For any state-action pair  $(s, a) \in$   
 656  $\mathcal{S} \times \mathcal{A}$ , with state action distribution  $d^\pi(s', a'|s, a) = \frac{1}{1-\gamma} \sum_{t=0}^{\infty} \gamma^t p^\pi((s, a) \rightarrow s', t) \pi(a'|s')$ , the  
 657 value error  $\Delta_Q(s, a)$  can be defined as a function of the Bellman error  $\epsilon_Q$*   
 658

659 
$$\Delta_Q(s, a) = \frac{1}{1-\gamma} \mathbb{E}_{(s', a') \sim d^\pi(\cdot | s, a)} [\epsilon_Q(s', a')]. \quad (14)$$
  
 660

661 *Proof.* We begin by stating results from Kakade & Langford (2002); Schulman (2015); Queeney  
 662 et al. (2021). A policy  $\pi$  induces a normalized discounted state visitation distribution  $d^\pi$ , where  
 663  $d^\pi(s'|s, a) = \frac{1}{1-\gamma} \sum_{t=0}^{\infty} \gamma^t p^\pi((s, a) \rightarrow s', t)$ . We write the corresponding normalized discounted  
 664 state-action visitation distribution as  $d^\pi(s', a'|s, a) = d^\pi(s'|s, a) \pi(a' | s')$ , where we make it clear  
 665 from the context whether  $d^\pi$  refers to a distribution over states or state-action pairs.  
 666

667 First by definition, for state  $s_1$  and action  $a_1$ , we have:  
 668

669 
$$\mathbb{E}_{d^\pi} [\epsilon(s_1, a_1)] \quad (15)$$
  
 670

671 
$$= \sum_{s_1} d^\pi(s_1) \sum_{a_1} \pi(a_1 | s_1) \epsilon(s_1, a_1). \quad (16)$$

672 
$$= (1-\gamma) \mathbb{E}_\pi \left[ \sum_{t=0}^{\infty} \gamma^t (Q(s_t, a_t) - r(s_t, a_t) - \gamma Q(s_{t+1}, a_{t+1})) \right] \quad (17)$$
  
 673

674 
$$= (1-\gamma) \mathbb{E}_\pi \left[ Q(s_0, a_0) - \sum_{t=0}^{\infty} \gamma^t r(s_t, a_t) \right] \quad (18)$$
  
 675

676 
$$= (1-\gamma)(Q(s_0, a_0) - Q^\pi(s_0, a_0)) \quad (19)$$
  
 677

678 Then, we can derive similar result when we have state  $s_{k+1}$  and action  $a_{k+1}$ ,  
 679

680 
$$\mathbb{E}_{d^\pi} [\epsilon(s_{k+1}, a_{k+1})] = (1-\gamma)(Q(s_k, a_k) - Q^\pi(s_k, a_k)) \quad (20)$$
  
 681

682 Finally, we have that:  
 683

684 
$$\frac{1}{1-\gamma} \mathbb{E}_{(s', a') \sim d^\pi(\cdot | s, a)} [\epsilon(s', a')] = Q(s, a) - Q^\pi(s, a) = \Delta_Q(s, a)$$
  
 685

686  $\square$   
 687

688 **A.2 PROOF OF PROPOSITION 4.3**  
 689

690 **Proposition 4.3 (Bias stems from accumulated Bellman errors.)** *For any state-action pair  
 691  $(s_0, a_0) \in \mathcal{S} \times \mathcal{A}$ , the value error  $\Delta_Q(s_0, a_0)$  is the accumulation of the Bellman errors  $\epsilon_Q$  over  
 692 future time steps:*  
 693

694 
$$\Delta_Q(s_0, a_0) = \epsilon_Q(s_0, a_0) + \mathbb{E}_\pi \left[ \sum_{t=1}^{\infty} \gamma^t \epsilon(s_t, a_t) \right] \quad (21)$$
  
 695

696 *Proof.* First by definition:  
 697

698 
$$\Delta(s, a) := Q(s, a) - Q^\pi(s, a) \quad (22)$$
  
 699

700 
$$\Rightarrow Q^\pi(s, a) = Q(s, a) - \Delta(s, a). \quad (23)$$
  
 701

702 Then we can decompose value error:  
 703

$$\Delta(s, a) = Q(s, a) - Q^\pi(s, a) \quad (24)$$

$$= Q(s, a) - (r(s, a) + \gamma \mathbb{E}_\pi[Q^\pi(s', a')]) \quad (25)$$

$$= Q(s, a) - (r(s, a) + \gamma \mathbb{E}_\pi[Q(s', a') - \Delta(s', a')]) \quad (26)$$

$$= Q(s, a) - (r(s, a) + \gamma \mathbb{E}_\pi[Q(s', a')]) + \gamma \mathbb{E}_\pi[\Delta(s', a')] \quad (27)$$

$$= \epsilon(s, a) + \gamma \mathbb{E}_\pi[\Delta(s', a')] \quad (28)$$

$$\vdots \quad (29)$$

$$= \epsilon(s, a) + \gamma \mathbb{E}_\pi[\epsilon(s', a')] + \gamma^2 \mathbb{E}_\pi[\Delta(s'', a'')]. \quad (30)$$

714 Finally, we derive:  
 715

$$\Delta_Q(s_0, a_0) = \epsilon_Q(s_0, a_0) + \mathbb{E}_\pi \left[ \sum_{t=1}^{\infty} \gamma^t \epsilon(s_t, a_t) \right].$$

716  $\square$   
 717  
 718  
 719  
 720

## 721 B ALGORITHM

723 MRT initialize two Bellman iteration process, One is used for predict the bias of Bellman error, and  
 724 the other one is used for learning an accurate value function with bias reduction from the Bellman  
 725 error. Our method can seamlessly integrate with any DRL algorithm. In practice, after predicting  
 726 the bias, we allocate a certain number of time steps for the  $Q_2$  function in Eq. 13 to learn. After  
 727 these time steps, we synchronize the parameters of  $Q_2$  with  $Q_1$  and the target network.

---

### 729 Algorithm 1 Monotonic increasing linear Reward Transformation (MRT).

730 **Require:**  $\theta, \bar{\theta}, \phi$ , Replay Buffer  $D$   $\triangleright$  Initial parameters  $\theta, \bar{\theta}$  of the  $Q$  function and  $\phi$  of the target  
 731 policy  $\pi_\phi$ .

732 1:  $\check{\theta} \leftarrow \theta, \mathcal{D} \leftarrow \emptyset$   $\triangleright$  Initialize parameters  $\check{\theta}$  of target Q-network

733 2: **for** each iteration **do**

734 3:   **for** each environment step **do**

735 4:     Run policy  $\phi$  in environment to collect transitions

736 5:     Store transitions into Buffer  $D$

737 6:   **end for**

738 7:   **for** each training step **do**

739 8:     sample batch transition  $(s, a, r, s')$  from Buffer

740 9:     update policy  $\phi$  according to any DRL algorithm

741 10:    for each transition, compute the TD error

742 11:    update  $\theta$  by minimizing the batch TD error

743 12:    estimated the bias with the TD error periodically

744 13:    update  $\bar{\theta}$  with bias reduction target Q-value

745 14:   **end for**

746 15:     $\check{\theta} \leftarrow \tau \bar{\theta} + (1 - \tau) \check{\theta}, \theta \leftarrow \tau \bar{\theta} + (1 - \tau) \theta$

747 16: **end for**

748 **Ensure:**  $\phi$   $\triangleright$  Optimized policy

---

749 In this paper, we do not specifically discuss the initialization of the  $Q$ -function or policy, as these  
 750 steps have already been addressed in previous studies Haarnoja et al. (2018a). To apply our method  
 751 to any DRL algorithm, the relative changes are as follows: in line 12, we estimate the bias of  
 752 the Bellman error; in line 13, we update the low-variance  $Q$ -function; and in line 15, we adopt  
 753 delayed updates to synchronize the parameters of the low-variance  $Q$ -function with those of other  
 754  $Q$ -functions. To maintain logical clarity, we simplify the representation of the target  $Q$ -function.  
 755 The target  $Q$ -function may have multiple forms, as seen in the TD3 Fujimoto et al. (2018) paper. We  
 clarify this detail here.

756 **C DETAIL NUMERICAL RESULT**  
 757  
 758

759 Some results in the figure are not very clear due to differences in data scales and overlapping curves,  
 760 making comparisons less obvious. To provide a clearer analysis, we have reorganized all the results  
 761 into a table, recording outputs every 0.2 million steps. The detailed results are shown in Table 1.  
 762 The data in the table represent the mean of six results, along with one standard deviation, covering  
 763 a 95% confidence interval. The best results are highlighted in bold.  
 764  
 765  
 766

767 Table 1: Numerical Result of Average Episodic Reward. (A) Humanoid-v4 (B) HumanoidStandup-  
 768 v4 (c) Ant-v4 (D) HalfCheetah-v4 (E) Hopper-v4 (F) Swimmer-v4

Env	Algo	0.2M	0.4M	0.6M	0.8M	1M
(A)	TD7	<b>2967.72 ± 1150.24</b>	4822.53 ± 2116.07	6513.07 ± 340.57	6648.29 ± 713.04	6714.27 ± 619.08
	TD7+MRT	2688.12 ± 1653.01	<b>6053.62 ± 964.87</b>	<b>6831.41 ± 419.09</b>	<b>7124.76 ± 438.29</b>	<b>6902.72 ± 1663.1</b>
	RRS	737.9 ± 201.42	3268.5 ± 1601.4	5065.71 ± 146.34	5091.56 ± 173.47	5183.52 ± 171.04
	RRS+MRT	782.18 ± 221.26	4277.43 ± 1115.75	4893.84 ± 532.89	4827.64 ± 1012.94	5132.51 ± 560.97
	TD3	875.45 ± 405.8	2596.93 ± 1302.98	4517.56 ± 704.81	4925.12 ± 271.16	5158.17 ± 245.98
	TD3+MRT	677.92 ± 39.98	3186.55 ± 1645.28	4923.43 ± 221.93	4879.45 ± 309.63	5263.84 ± 187.92
(B)	TD7	151725.22 ± 6682.32	159877.79 ± 2716.19	159979.43 ± 3166.79	160650.85 ± 1843.46	161599.67 ± 2129.93
	TD7+MRT	<b>155146.12 ± 10903.61</b>	<b>160334.25 ± 9870.83</b>	<b>182681.5 ± 32419.07</b>	<b>177913.47 ± 24701.51</b>	<b>172663.08 ± 15063.59</b>
	RRS	88700.35 ± 9331.45	89977.85 ± 9127.66	88891.87 ± 8366.44	91862.05 ± 5984.5	93510.03 ± 5916.96
	RRS+MRT	102863.1 ± 16483.1	102950.0 ± 16465.94	102764.39 ± 16514.43	102804.6 ± 16129.92	103059.35 ± 16439.05
	TD3	97760.89 ± 21166.12	97894.46 ± 21151.11	97995.46 ± 20865.68	98024.74 ± 21252.07	98259.45 ± 20689.53
	TD3+MRT	104253.44 ± 17759.69	103224.3 ± 17674.67	104419.95 ± 17800.85	105520.74 ± 18392.09	105509.46 ± 18378.86
(C)	TD7	5066.0 ± 1385.38	6832.59 ± 708.66	<b>8255.37 ± 622.25</b>	7819.47 ± 1099.33	8079.26 ± 933.06
	TD7+MRT	<b>5999.98 ± 511.31</b>	<b>7214.9 ± 198.13</b>	7893.69 ± 354.34	<b>8217.03 ± 726.93</b>	<b>8781.44 ± 694.34</b>
	RRS	1161.07 ± 395.87	3107.51 ± 1207.38	3895.63 ± 1632.36	4318.46 ± 1722.3	4467.62 ± 1751.35
	RRS+MRT	1386.77 ± 843.81	3547.72 ± 1141.62	4994.54 ± 189.86	4678.93 ± 1113.55	5529.2 ± 201.36
	TD3	1136.5 ± 373.53	1963.78 ± 1275.9	2884.04 ± 1501.95	3342.98 ± 1537.06	3734.29 ± 1478.07
	TD3+MRT	1046.96 ± 274.71	2433.53 ± 1508.08	2771.54 ± 1600.17	3433.58 ± 1499.59	3972.38 ± 1357.83
(D)	TD7	12461.65 ± 1131.17	<b>16104.55 ± 593.02</b>	16720.68 ± 208.9	17244.15 ± 182.15	<b>17291.41 ± 200.61</b>
	TD7+MRT	<b>12995.64 ± 633.1</b>	16036.93 ± 761.71	<b>16958.32 ± 307.61</b>	<b>17387.21 ± 258.62</b>	17267.75 ± 215.09
	RRS	6432.43 ± 570.43	8148.57 ± 1190.63	9172.71 ± 1223.24	10198.72 ± 1198.15	10551.27 ± 1215.57
	RRS+MRT	6465.94 ± 426.35	8209.68 ± 1096.54	9359.76 ± 1140.33	10678.88 ± 655.21	11255.05 ± 593.87
	TD3	6585.94 ± 481.08	8670.89 ± 805.42	9582.96 ± 769.87	10054.63 ± 764.89	10590.11 ± 723.63
	TD3+MRT	6789.49 ± 356.01	9055.14 ± 522.3	10188.93 ± 543.87	10186.0 ± 987.97	11179.5 ± 491.82
(E)	TD7	<b>2529.54 ± 843.66</b>	2379.75 ± 884.58	3189.78 ± 575.91	3286.19 ± 800.75	2410.19 ± 961.2
	TD7+MRT	2445.37 ± 1162.01	2509.6 ± 945.57	2571.26 ± 747.59	2812.32 ± 749.38	3076.99 ± 940.72
	RRS	1151.63 ± 761.39	2505.71 ± 983.89	<b>3375.09 ± 107.06</b>	3400.35 ± 153.31	2691.38 ± 1147.2
	RRS+MRT	1741.77 ± 1120.7	<b>3338.48 ± 165.87</b>	3251.63 ± 344.11	<b>3494.09 ± 81.85</b>	<b>3537.2 ± 56.93</b>
	TD3	1331.36 ± 1069.89	1962.45 ± 1203.24	2545.1 ± 1201.5	2025.49 ± 993.43	3118.38 ± 518.57
	TD3+MRT	890.19 ± 762.45	2014.25 ± 1052.76	2394.97 ± 1033.55	2815.3 ± 850.2	3378.25 ± 105.71
(F)	TD7	70.94 ± 23.5	104.81 ± 12.73	<b>118.34 ± 5.57</b>	<b>123.28 ± 12.0</b>	114.36 ± 16.28
	TD7+MRT	<b>99.95 ± 24.68</b>	<b>107.13 ± 31.74</b>	95.76 ± 32.4	118.33 ± 24.88	<b>128.21 ± 8.79</b>
	RRS	44.36 ± 4.58	58.5 ± 19.7	73.61 ± 22.92	88.23 ± 25.78	99.72 ± 31.57
	RRS+MRT	48.2 ± 7.84	48.59 ± 6.51	76.83 ± 15.84	100.01 ± 18.17	112.91 ± 10.89
	TD3	50.9 ± 6.33	75.05 ± 22.54	90.11 ± 21.14	98.72 ± 24.15	96.13 ± 25.5
	TD3+MRT	50.78 ± 9.35	64.27 ± 45.49	98.64 ± 25.56	98.18 ± 28.36	112.67 ± 12.8

793 From the table, we can observe that the training stability of TD7 is not ideal in certain environments.  
 794 For example, the final converged result is sometimes worse than the maximum value achieved during  
 795 training, which affects the stability of our method on TD7 as well. The fundamental reason for  
 796 this issue lies in the TD7 algorithm’s weighted sampling of experience replay based on TD error,  
 797 without considering the impact of weighting on convergence. This can be seen from the data at  
 798 different training stages. For instance, in the HumanoidStandup-v4 environment, the best result for  
 799 the TD7+MRT algorithm appears at 0.6M time steps. Similarly, in the Ant-v4 environment, TD7  
 800 achieves its best result at 0.6M time steps.  
 801  
 802

803 **D HYPER-PARAMETERS**  
 804  
 805

806 Taking the TD3 algorithm as an example, MRT introduces only one additional hyperparameter—the  
 807 period for estimating the bias.  
 808  
 809

810

811

Table 2: Hyper-parameters

812

813

814

815

816

817

818

819

820

821

822

823

824

825

826

827

828

829

830

831

## E MORE EXPERIMENTS

832

833

## E.1 THE IMPACT OF BIAS REDUCTION ON EXPLORATION

834

835

836

837

Exploration is also crucial in reinforcement learning. While bias reduction serves as an optimization technique, examining its impact on exploration provides indirect insight into how bias reduction affects policy learning. In most cases, a good policy naturally leads to effective exploration, although effective exploration does not necessarily guarantee stable convergence.

838

839

We have recorded the results of exploration, as shown in Fig. 4.

840

841

842

843

844

845

846

847

848

849

850

851

852

853

854

855

856

857

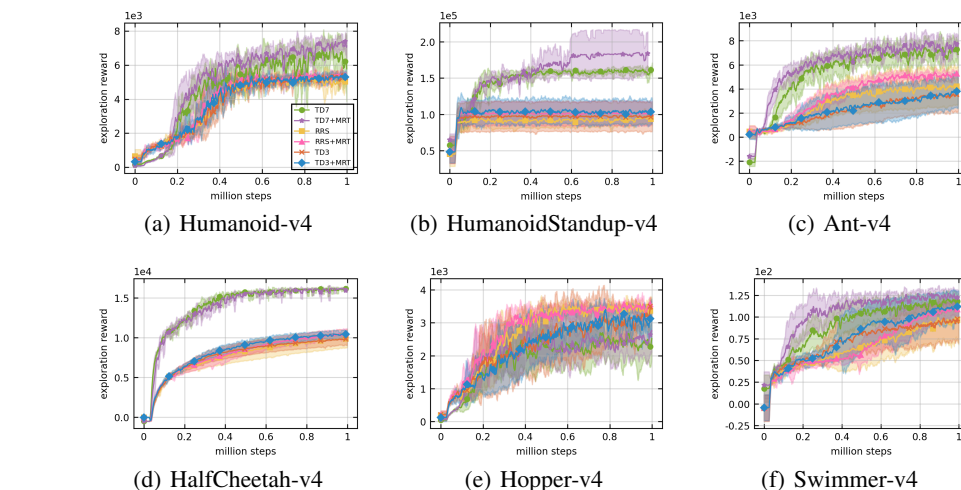


Figure 4: Exploration reward of all algorithms. The x-axis represents time steps, with one million interaction steps, and the y-axis represents the average episodic exploration reward.

858

859

860

861

862

863

From Fig. 4, we observe that after applying the MRT method, the exploration performance is almost consistently better than that of the baseline algorithms. This aligns with the policy evaluation results, particularly in the Humanoid-v4, HumanoidStandup-v4, and Ant-v4 environments, where the exploration performance continues to improve. This also explains why Bellman error contin-

864      ues to increase in the later stages of training. Bias reduction enables a smoother learning process  
865      for Q-values, reducing the time required for value fitting and allowing additional opportunities for  
866      exploration. This additional exploration leads to better policies, which in turn enhance the value of  
867      earlier states and increase Q-value errors—ultimately resulting in improved performance.  
868

## 869      F LIMITATION 870

871      In terms of computational efficiency, our method introduces an additional Q-function update, which  
872      can potentially increase computational cost. Although compared to prior methods such as the RRS  
873      algorithm, our approach uses fewer Q-functions overall, this added update still contributes to higher  
874      computation overhead. Specifically, if we consider the cost of Q-function computation alone, and  
875      take the original DQN algorithm as a baseline, DQN only computes a single target Q-function and  
876      updates the current Q-function once per step. TD3 computes two target Q-functions and updates  
877      the current Q-function once. TD3+MRT adds one more Q-function update on top of TD3. In  
878      our method, while we maintain a relatively efficient structure, the additional Q-function update  
879      introduces a similar level of computational cost. Furthermore, we periodically approximate the bias  
880      of the Bellman error in our method. However, this estimation may be inaccurate in some situations.  
881      We assume that Q-values are overestimated, but the extent of this overestimation and the frequency  
882      at which it occurs are difficult to determine precisely.  
883  
884  
885  
886  
887  
888  
889  
890  
891  
892  
893  
894  
895  
896  
897  
898  
899  
900  
901  
902  
903  
904  
905  
906  
907  
908  
909  
910  
911  
912  
913  
914  
915  
916  
917